Intramolecular non-covalent isotope effects at natural abundance associated with the migration of paracetamol in solid matrices during liquid chromatography

Maxime Julien, Mathilde Liégeois, Patrick Höhener, Piotr Paneth, Gérald Remaud

Intramolecular non-covalent isotope effects at natural abundance associated with the migration of paracetamol in solid matrices during liquid chromatography

Maxime Julien*[1,2], Mathilde Liégeois[2], Patrick Höhener[3], Piotr Paneth[4], Gérald S. Remaud[2]

[1]Department of Earth and Planetary Sciences, Tokyo Institute of Technology, 2-12-1 Ōokayama, Meguro-ku, Tokyo 152-8551 Japan.

[2] Université de Nantes, CNRS, CEISAM UMR 6230, F-44000 Nantes, France.

[3] University of Aix-Marseille-CNRS, Laboratoire Chimie Environnement – UMR 7376, place Victor Hugo 3, 13331 Marseille, France.

[4] Institute of Applied Radiation Chemistry, Lodz University of Technology, Zeromskiego 116, 90-924 Lodz, Poland

Correspondence: M. Julien; e-mail: julien.m.aa@m.titech.ac.jp

Abstract

Position-specific isotope analysis by Nuclear Magnetic Resonance spectrometry was employed to study the ^{13}C intramolecular isotopic fractionation associated with the migration of organic substrates through different stationary phases. Liquid chromatography is often used to isolate compounds prior to their isotope analysis and this purification step potentially alters the isotopic composition of target compounds introducing a bias in the later measured data. Moreover, results from liquid chromatography can yield the sorption parameters needed in reactive transport models that predict the transport and fate of organic contaminants to in the environment. The aim of this study was to use intramolecular isotope analysis to study both ^{13}C and ^{15}N isotope effects associated with the migration of paracetamol through different stationary phases and to compare them to effects observed previously for vanillin. Results showed very different intramolecular isotope fractionation profiles depending on the chemical structure of the stationary phase. The data also demonstrate that both the amplitude and the distribution of measured isotope effects depend on the nature of the non-covalent interactions involved in the migration process. Results provided by theoretical calculation performed during this study also confirmed the direct link between observed intramolecular isotope fractionation and the nature of involved intermolecular interactions. It is concluded that the nature of the stationary phase through which the substrate passes has a major impact on the intramolecular isotopic composition of organic compounds isolated by chromatography methods. These findings allow to better understand the fate of organic contaminants undergoing reactive transport in soils or aquifers.

Keywords:

Position-specific isotope effects – isotope enrichment factor – migration – paracetamol – Rayleigh equation – irm-^{13}C NMR– DFT calculations

1. Introduction

Liquid chromatography, commonly used to isolatee compounds from a complex mixture, is known to create isotope effects. The non-covalent interactions settled between the solid phase and the substrate during the migration are isotopically selective resulting in isotopic fractionation of the migrating compounds. The link between these interactions and the associated non-covalent isotope effects (NCIEs) remains poorly documented [1–3]. Understanding the isotopic fractionation processes associated with chromatography is of primary importance for correcting further isotopic measurements when used during the sample preparation and/or the direct coupling of isotope ratio monitoring by Mass Spectrometry (irm-MS, known also as IRMS: Isotope Ratio by Mass Spectrometry) with high-performance liquid chromatography (HPLC) [4] or gas chromatography (GC) [5,6]. Moreover, liquid chromatography (and more generally sorption experiments) are used for modeling the migration of organic compounds in environment to determine the impact of this process on considered pollutants isotopic composition and to study their origins and fate [7,8].

It is difficult to study migration mechanisms and understand their associated isotope fractionations of a pollutant in environment studies, as example. Indeed, this phenomenon involves different processes such as advection, diffusion/dispersion and sorption. Advection

refers to the transport of a compound depending on the ground relief or the presence of a stream (air, water) in the considered polluted site. It corresponds to the movement of a contaminant plume in the soil or in water) and does not depend on the chemical composition, so it is considered as inert in terms of isotope fractionation. Diffusion and dispersion define the way a contaminant will spread in the environment and may contribute to isotope fractionation. However, these fractionations are considered to be small or non-significant in advection-dominated transport situations and for experiments with short durations [9–11]. By contrast, the sorption/desorption processes occurring during the migration directly involve intermolecular non-covalent interactions, which have already been proven to be associated with intramolecular ^{13}C isotope effects, i.e. position-specific ^{13}C fractionation [12]. Furthermore, different types of intermolecular interactions (hydrogen bonds, van der Waals, π-stacking, halogen bonds) can be observed during migration depending on the molecular structures of both the contaminant and the solid matrix resulting in variable isotope effects.

The isotope fractionations and the calculation of the associated isotopic effects provide information on the intensity of interactions between the solute and the solid matrix. Most isotope studies are performed using irm-MS targeting mostly ^{13}C and ^{2}H in organic contaminants [8,13] and moreover on enriched material for the chromatography investigations [1–3]. However, this method only provides a measurement of the average isotopic composition, which is the mean value of isotope ratios of all carbon or hydrogen positions within the considered molecule. Using this method, isotopologues (two molecules with a different number of heavy atoms, see section 3.1 for further definition) that react differently with the considered stationary phase will elute separately [14]. Fully deuterated compounds can be separated from their protiated counterparts

by liquid [3] or gas chromatography [15], for example. To access the intramolecular ^{13}C information without prior (bio)chemical degradation of the target compound, a small number of position-specific isotope analysis (PSIA) techniques have been developed such as isotope ratio monitoring by ^{13}C Nuclear Magnetic Resonance (irm-^{13}C NMR) [16–18], on-line pyrolysis coupled with irm-MS [19–22] and high-resolution irm-MS [23,24]. All these techniques make it possible to identify which isotopomer (two molecules with the same amount of heavy atom but located on different position) preferentially interacts during the studied process [14]. PSIA using irm-^{13}C/^{15}N NMR has been successfully used to reveal intramolecular NCIE during chromatographic elution on normal phase for ^{13}C [12,25] and ^{15}N [26] or inverse phase for ^{13}C [27]. Furthermore, this approach was able to found a possible link between the magnitude of fractionation and the strength of intermolecular interactions within a liquid during the liquid-vapor transition as evaporation of VOCs for ^{13}C [28,29] or distillation for ^{2}H and ^{13}C [14,30].

In the present study, ^{13}C intramolecular isotope analysis using irm-^{13}C NMR was employed to observe the position-specific isotope effects (PSIEs) associated with the chromatographic elution on several stationary phases. The potential connection between the magnitude of fractionation and strength of interaction between organic solute and solid phase is expected to provide insights about how different types of matrices could retain organic chemicals. Isotope fractionation associated with migration of organic contaminants were largely studied using deuterated compounds [1–3]. However, only few works looked at isotopes at natural abundance and the influence of migration on isotope composition is still debated. As an example, the migration of BTEX (Benzene, Toluene, Ethylbenzene, Xylenes) on reverse phase HPLC did not show any significant IE for ^{13}C at the global level [31], nor did the migration of BTEX and MTBE on HPLC

using humic acid as stationary phase [32]. Some sorption experiments of BTEX and chlorinated solvents on activated charcoal also showed non-significant IEs for global ^{13}C and ^{2}H compositions [33,34]. Nevertheless, some other experiments highlighted the presence of ^{13}C and ^{2}H isotope fractionation during sorption/desorption cycles of BTEX on different adsorbing materials, still using average isotope parameters [35], which encouraged us to undertake further experiments probing PSIA because the small detected IEs may be composed by counteractive normal and inverse IEs within the studied molecules resulting in the measurement of low or non-significant global isotope effects, i.e. using irm-^{13}C MS. The concomitance of normal and inverse isotope effects within the same molecule was already detected during the migration of vanillin and derivatives on both normal phase silica gel (SG) and reverse phase (RP) [12,25]. The results of these works were presented as a qualitative description of the ^{13}C intramolecular fractionations observed, with no enrichment factor calculated. Although, isotope fractionation of vanillin migrating on RP was further studied to develop a reactive transport capable of predicting the position-specific isotopic fractionation behavior of this compound in the environment [27].

As soil composition is very variable and not homogeneous, we have chosen to study the migration of paracetamol through different pure materials using liquid chromatography and to measure associated intramolecular ^{13}C and ^{15}N IEs. Four model materials with various chemical compositions were used as stationary phase in this study: silica gel normal phase (SG), cellulose (CE), activated charcoal (AC) and silica gel C8-reversed phase (RP). The choice of the solute and these solid matrices will be further rationalized in the section 3, as well the role of the eluent that is important in the selection of the isotopomers during the elution [1–3]. Thus, it is expected that different types of non-covalent intermolecular interactions contribute in the PSIF. The

130 determination of the enrichment factor at each carbon position should help in the evaluation of
131 the strength of these interactions. That is the reason why we have performed these calculations
132 from previous published data of vanillin eluted through normal phase silica gel [12] and reversed
133 phase silica gel [27] to better highlight the role of non-covalent interactions in intramolecular
134 isotope fractionations occurring during the migration. In addition, quantum mechanical
135 calculations for the transition of paracetamol from diethyl ether (low polarity) to acetone
136 (moderate polarity) or water (polar compound) were performed during this study. These
137 theoretical data should help better understanding the effect of hydrogen-bonding and, more
138 generally, the polarization on measured PSIEs associated with the migration.

139

140 **2. Materials and Methods**

141 *2.1. Chemicals*

142 Paracetamol ($C_8H_9NO_2$, CAS-Number 103-90-2), silica gel high-purity grade, average pore size 60
143 Å (52-73 Å), 70-230 mesh, 63-200 µm, silica gel C8-reversed phase, and activated charcoal were
144 purchased from Sigma Aldrich. Cellulose was obtained from Fluka-chemicals and DMSO-d_6 was
145 purchased from Eurisotop. Acetone and diethyl ether used as eluent were from Sigma Aldrich as
146 HPLC quality, without further purification.

147 *2.2. Chromatographic procedures*

148 In order to determine both ^{13}C and ^{15}N isotope fractionation occurring during the migration of
149 paracetamol through different materials, liquid chromatography experiments were performed
150 using 4 different stationary phases (separately): normal phase silica gel (SG), silica gel C8-reversed

phase (RP), cellulose (CE) and activated charcoal (AC). For each experiment the amount of material was adapted in order to obtain around 250 mm of stationary phase in a chromatography column (internal diameter 40 mm except for silica gel C8-reversed phase which was 30 mm). Then the protocol was the same for all types of stationary phase: (i) 2 g of pure paracetamol was introduced as a powder at the top of the column and gently mixed with the first 20 mm of the stationary phase to start the migration; (ii) The elution was performed using a mixture of 90% of diethyl ether and 10% acetone, as acetone solubilizes well paracetamol to some extent [36], while it is almost totally non-soluble in ether that is used to decrease the polarity of acetone, avoiding thus, a too rapid elution of paracetamol and (iii) it was collected in 4 fractions (approx. 500 mg each). The exact amount of each fraction was determined by weighting the eluted paracetamol after evaporation of the solvents to dryness and the corresponding percentage of introduced paracetamol was calculated (see Table 2). The starting paracetamol and the 4 samples obtained from elution of each stationary phase chromatography were analyzed for their isotopic parameters.

2.3. Global ^{13}C and ^{15}N isotope analysis

Carbon ($^{13}C/^{12}C$) and nitrogen ($^{15}N/^{14}N$) global isotope ratio measurements, expressed in delta notation ($\delta^{13}C_g$ and $\delta^{15}N_g$ (‰)), were determined by irm-MS using an Integra2 spectrometer (Sercon Instruments, Crewe, UK) linked to a Sercon elemental analyzer (EA) fitted with an autosampler (Sercon Instruments, Crewe, UK). About 1 mg of sample was sealed in a tin capsule. $\delta^{13}C_g$ and $\delta^{15}N_g$ of the resulting gases, CO_2 and N_2 were determined by reference to a working standard of glutamic acid standardized against calibrated international reference material (IAEA-

CH6 and IAEA-CH7 for carbon isotope ratio and IAEA-N1 and IAEA-N2 for nitrogen isotope ratio). The ^{13}C and ^{15}N global isotope compositions of the whole molecule were calculated from:

$$\delta^{A}X\ (‰) = \left(\frac{R}{R_{Std}} - 1\right) \times 1000 \qquad \text{eq. 1}$$

Where ^{A}X stands for either ^{13}C or ^{15}N, R is the isotope ratio of the sample and R_{std} is the isotope ratio of Vienna Pee Dee Belemnite reference standard (V-PDB) for ^{13}C (R_{std} = 0.0112372) or atmospheric air for ^{15}N (R_{std} = 0.003677).

2.4. Intramolecular ^{13}C isotope analysis by irm-^{13}C NMR

PSIA of paracetamol using irm-^{13}C NMR was described in a previous study [37]. The sample preparation consisted in the successive addition in a 4 mL vial of 250 mg of paracetamol and 600 µL of DMSO-d_6. The respective amount of each was adapted according to (i) the T1 values (longitudinal relaxation), (ii) the solubility in the deuterated solvent and (iii) the ^{13}C NMR spectrum: no peak overlapping (see Figure S3). Irm-^{13}C NMR spectra were recorded using an AVANCE I 400 spectrometer (Bruker Biospin, Wissembourg, France), fitted with a 5 mm i.d. $^{1}H/^{13}C$ dual^{+} probe, carefully tuned at the recording frequency of 100.61 MHz. The temperature of the probe was set to 303 K, without tube rotation. The exact NMR acquisition conditions are detailed in the SI. Isotope ^{13}C compositions were calculated from processed spectra as described previously [38]: further details are given in the SI (Table S2).

2.5. Calculation of enrichment factors (ε) and associated expanded uncertainty (U)

Enrichment factors (ε in ‰) is a common way used to express IEs. An isotope effect is considered as normal (light isotopologues respond preferentially) when $\varepsilon < 0$ and inverse when $\varepsilon > 0$.

Enrichment factors were determined using Rayleigh plots in which ln(*f*) is plotted on the x-axis (where *f* is the fraction of paracetamol remaining in the column) and ln(R/R_0) on the y-axis (eq. 2 and 3, R is the isotope ratio of the sample and R_0 the isotope ratio of paracetamol at t_0) [39,40].

$$\ln\left(\frac{R}{R_0}\right) = (\alpha - 1) \times \ln(f) \quad \text{eq. 2}$$

$$\varepsilon = (\alpha - 1) \times 1000 \quad \text{eq. 3}$$

In Rayleigh plots, the slope of the trend line corresponds to the enrichment factor (ε) and the associated root mean square (R^2) gives a first indication of the quality of the linearity. However, in order to determine the significance threshold of the enrichment factor, the expanded uncertainty needs to be calculated. The determination of the expanded uncertainty associated with the enrichment factor determined using the Rayleigh-plot can be directly calculated using the function "LINEST" in Microsoft Excel™, as previously described [39,41]. This function calculates both the slope and the standard deviation of the trend line (STDV slope). The expanded uncertainty can thus be calculated as follows (eq. 4):

$$U = k \times \text{STDV slope} \quad \text{eq. 4}$$

where k = 2 for a coverage factor at the 95% confidence level according to Student's *t*-distribution.

In this context, data are presented as $\varepsilon \pm U$ and enrichment factors are considered as significant when $|\varepsilon| > U$.

2.6. Theoretical calculation of enrichment factors (ε)

We have used two models of the environment. The first one involved a SMD continuum solvent model [42], which uses bulk properties of the solvent to create a dielectric cavity in which the

212 solute is immersed. In the second approach, explicit solvent molecules are used. Within this
213 approach we have used 14 water molecules comprising the first solvation shell of paracetamol
214 (see Figure 1) as a model of well-defined, strong hydrogen bonding network with availability of
215 both proton donor and proton acceptor sites. Calculations were carried out at the DFT level of
216 theory, using ωB97X-D functional [43] expressed in the def2-TZVP basis set [44] as implemented
217 in the Gaussian16 program [45], which proved successful in our recent studies on vapor pressure
218 isotope effects of ethanol [46].

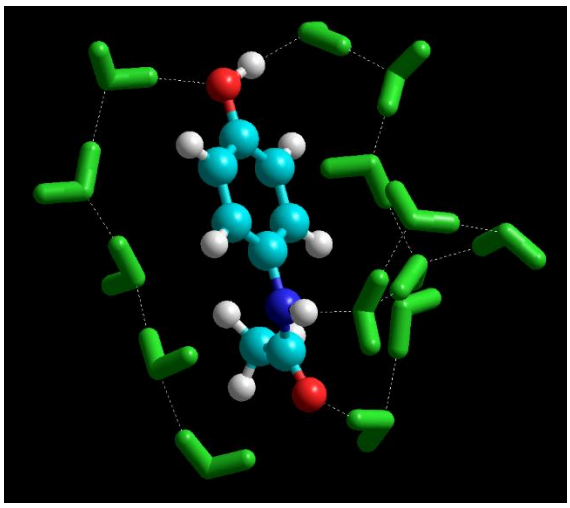

219

220 **Figure 1:** Solvent network around paracetamol molecule.

221 We have carried out calculations for structures of paracetamol in the gas phase, continuum
222 solvent models of diethyl ether and acetone, and surrounded by 14 explicitly treated water
223 molecules. For the optimized structures frequency calculations were carried out to ensure they
224 represent local minima, and for calculations of isotope effects (which were subsequently
225 converted into isotopic enrichment factors) using the Isoeff program [47].

226

3. Results and Discussion

3.1. Design of the experiments: choices of solid phases and solute

The goal of the work being double: (i) relationship between the type of stationary phase and the NCIE for a given chemical in liquid chromatography; and (ii) contribution to modelling the isotope fractionation upon migration of organic chemicals in a soil, the choice of the solid matrices and of the solute should be further explained. The relationship between structural substitutions and NCIE during the chromatographic elution on normal phase silica gel of a group of phenolic compounds related to vanillin was previously investigated on qualitative basis [12,25]. Herein one compound has been studied during elution on four stationary phases. This compound is paracetamol also called acetaminophen, it is one of the most widely used drugs in the world. Although this painkiller is a prodrug, which means that it needs to be partially metabolized in the liver to become active [48], large quantities of this whole molecule are found in the environment. Paracetamol can be converted into *N*-acetyl-*p*-benzoquinone imine and 1,4-benzoquinone in wastewater treatment plants by reacting with hypochlorite ions (ClO^-) [49]. These compounds are suspected to be genotoxic and mutagenic, so the monitoring of the fate of paracetamol is of primary importance [50–52].

Because of a high complexity, the NCIE during migration of paracetamol into a soil would difficult to interpret as the different sources of interaction nor their strengths between the chemical and the solid phase could be described. We opted to a differentiation of each category of forces responsible of the retention (or not) during the elution. As such, normal phase silica gel (SG) is both polar and hydrogen bond provider (silanol groups), cellulose is much less polar but still

248 provides hydrogen bonds (hydroxyl groups), the reverse C8 phase (RP) may be considered as
249 nonpolar and will favor weak forces (van der Waals), and finally the charcoal is well known to sorb
250 chemicals via π-ring current interactions. This diversity of dominating interactions for the studies
251 solid phases allowed us additionally to get a deeper insight into theoretical modelling of isotopic
252 fractionations using quantum-mechanical calculations.

253 The nature of the eluent is recognized as contributing to the elution order of the isotopomers. All
254 the studies of the isotope fractionation pointed out that the composition of solvents can change
255 the interactions between the solute and the solid phase. For the present work, the eluent has
256 been fixed at 10% of acetone and 90% of diethyl ether and the same for all experiments and
257 therefore for the four stationary phase. Paracetamol is not very soluble in all organic solvents and
258 is preferentially in alcohols. But the presence of strong hydrogen bonds via the hydroxyl groups
259 could annihilate other weak interactions. It is then expected that the isotope fractionation due to
260 weak interactions between paracetamol and the stationary phase could be observed. The mixture
261 of acetone (10%) and diethyl ether (90%) is polar enough to allow a chromatographic experiment
262 for the four solid phases with a gradual migration of paracetamol. Finally, being very volatile,
263 these solvents can be easily removed for each collected fraction leaving dry paracetamol for ^{13}C
264 NMR.

265 *3.2. What is measured by irm-^{13}C NMR and repeatability of the isotope compositions*

266 *3.2.1 Data obtained from isotopic NMR*

267 Even if several papers are now available in the literature [18,38,53], we think that it is worthwhile
268 to further describe the irm-^{13}C NMR methodology and the data it provides. Any molecules

containing isotopes are isotopologues, *i.e.* they have the same constitution and same configuration but differ in their isotope substitutions. Quantifying isotopologues having two or more heavy isotopes is not accessible for ^{13}C and ^{15}N, due their very low abundance, by current routine techniques as irm-MS or irm-NMR: the mono labelled, at natural abundance, molecules are considered. These molecules are named isotopomers, *i.e.* same chemical structure in which the heavy isotope differs as to its position in the structure. PSIA is therefore the approach consisting in the determination of the profile of isotopomers, as opposed to the quantitation of the mean ratio (bulk or global) of the ^{13}C isotopologues versus the light one (^{12}C). Irm-^{13}C NMR resolves fractionation of natural isotope values in ^{13}C for every position in the target molecules. For low isotopic abundance, as for natural-abundance ^{13}C (1.08%), molecules containing more than one ^{13}C are usually not detected by NMR. Therefore, each chemical shift (that is the peak in the spectrum, named *i*) corresponds to an isotopomer *i* (mono-labelled at natural abundance). Paracetamol has 8 carbon atoms at 6 specific positions (then 6 ^{13}C isotopomers numbered as described in Figure 2), and one nitrogen atom.

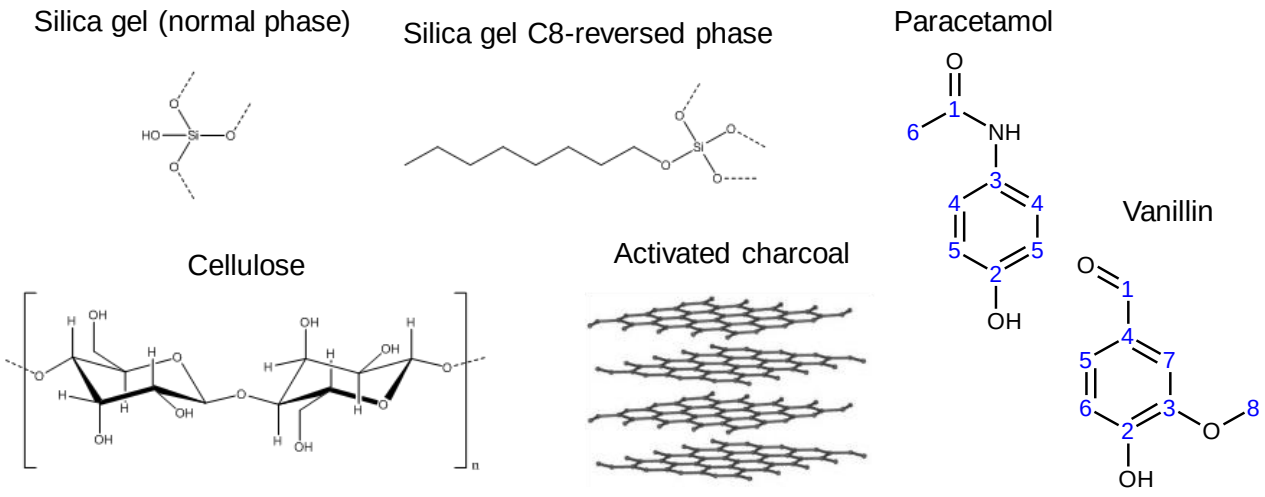

Figure 2: General chemical structure of the stationary phases employed in the present study. Also shown are the molecular structures of paracetamol and vanillin with the carbon atoms numbered in relation to decreasing ^{13}C chemical shift in the ^{13}C NMR spectrum.

The area S of the corresponding signal in the NMR spectrum is directly proportional to the amount of this isotopomer. The relationship between the mean and the position-specific ^{13}C content is found at the isotopic abundance *x* level: $x_i = x_g.f_i/F_i$ (Table 1). Thus irm-^{13}C NMR gives access to the relative intramolecular ^{13}C distribution, while irm-MS reports on the total amount of ^{13}C isotopes. Further details on the calculation of $\delta^{13}C_i$ are given in the SI.

Table 1: Symbols and their definitions used in the present work.

Symbol	**Definition**
$\delta^{13}C$	Carbon isotope composition: carbon isotopic ratio of the molecule relative to the international standard (Vienna Pee Dee Belemnite V-PDB)
$\delta^{13}C_g$	^{13}C mean isotopic composition of a whole molecule measured by irm-MS: global ^{13}C content. Also found as $\delta^{13}C_b$ for bulk value, or $\delta^{13}C_T$ for total value
$\delta^{13}C_i$	^{13}C isotopic composition of the carbon position *i* measured by PSIA (as irm-^{13}C NMR in this work)
$\Delta\delta^{13}C_g$	Difference between final $\delta^{13}C_g$ and initial $\delta^{13}C_g$
$\Delta\delta^{13}C_i$	Difference between final $\delta^{13}C_i$ and initial $\delta^{13}C_i$
f_i	Molar fraction for a carbon site *i* measured by irm-^{13}C NMR = area S of the peak corresponding to the carbon position *i* (S_i) divided by the sum of all the carbon sites of the molecule: $f_i = \frac{S_i}{\sum_n S_i}$.

F_i	Statistical molar fraction for a carbon site *i*: molar fraction for the carbon site *i* in cases of homogeneous ^{13}C distribution within the molecule (example: F_1 = 1/8 for paracetamol)
***f*i/*F*i**	Reduced molar fraction for a carbon *i*: any shift from 1 indicates an isotope fractionation
x	Isotopic abundance
ε_g	Enrichment factor calculated as described in the experimental section from $\Delta\delta^{13}C_g$
ε_i	Enrichment factor calculated as described in the experimental section from $\Delta\delta^{13}C_i$

Note: ^{15}N has only one possible position in paracetamol so only global analysis (irm-^{15}N MS) is done.

3.2.2 Precision of the isotopic compositions

The repeatability of both intramolecular and global isotope analysis was investigated. Data presented in Table 2 show a standard deviation (SD) of isotopic composition measurements comprised between 0.1 and 0.7‰. More interesting, global and intramolecular isotope compositions of material used as working reference were calculated using data from all collected fractions and the differences between these calculated values and direct measurements on the reference materials were calculated (see Table 2). These differences are comprised between 0.1 and 1.2‰ which confirms the repeatability and reproducibility of the isotope measurements (irm-EA/MS and irm-^{13}C NMR). Moreover, these data prove that differences in PSIEs discussed in this article are directly associated with the migration experiments and are not due to measurement error or a lack of recovery of the migrating material.

Table 2: Repeatability study of $\delta^{13}C_g$, $\delta^{15}N_g$ by irm-MS and intramolecular ^{13}C distribution measurements in paracetamol by irm-^{13}C NMR, $\delta^{13}C_i$ (SD = standard deviation), expressed in ‰. Also shown, the isotopic composition of material used as working reference calculated from values measured on the different fractions (see calculated) and the absolute difference with the direct measurement of paracetamol (see |difference|).

		$\delta^{13}C$ (‰)							$\delta^{15}N_g$ (‰)
	Experiment	**global**	**C-1**	**C-2**	**C-3**	**C-4**	**C-5**	**C-6**	
	1	-26.9	-32.4	-27.9	-34.9	-22.8	-21.6	-31.1	-3.7
	2	-26.9	-31.8	-26.3	-35.2	-23.1	-22.3	-31.2	-3.7
	3	-26.9	-31.6	-27.6	-34.1	-22.8	-22.0	-32.4	-3.8
	4	-26.9	-31.1	-26.9	-35.0	-22.9	-22.2	-32.1	-3.7
	5	-27.0	-32.3	-26.5	-34.5	-22.7	-22.7	-31.2	-3.7
	mean	-26.9	-31.9	-27.0	-34.7	-22.9	-22.2	-31.6	-3.7
	SD	0.1	0.5	0.7	0.4	0.2	0.4	0.6	0.1
SG	**calculated**	-27.6	-32.9	-28.1	-35.7	-23.7	-22.7	-30.9	-3.9
	|difference|	0.6	0.4	0.2	0.8	0.9	1.1	0.3	0.2
CE	**calculated**	-26.9	-32.4	-27.6	-34.7	-22.2	-22.3	-31.7	-3.9
	|difference|	0.0	0.0	0.3	0.2	0.6	0.6	0.5	0.1
AC	**calculated**	-27.1	-31.8	-27.6	-35.0	-23.2	-22.5	-31.3	-3.2
	|difference|	0.2	0.7	0.3	0.1	0.4	0.8	0.2	0.5
RP	**calculated**	-26.9	-32.0	-27.4	-34.0	-23.3	-22.5	-29.9	-3.6
	|difference|	0.0	0.5	0.5	0.9	0.5	0.9	1.2	0.1

3.3. ^{13}C and ^{15}N isotope effects

For each of the four migration experiments, global and ^{13}C intramolecular (carbon positions 1 to 6) data were plotted on the same graph in order to determine corresponding ε values and nitrogen data are presented in a separated graph (see Figure 3). The Rayleigh equation and, by extension, Rayleigh plot are usually employed to follow the evolution of the isotope ratio of a compound as a function of a reaction's progress. This equation allows calculating the fractionation factor created by a considered process such as a (bio)chemical reaction [39] or the migration during liquid chromatography in the present work.

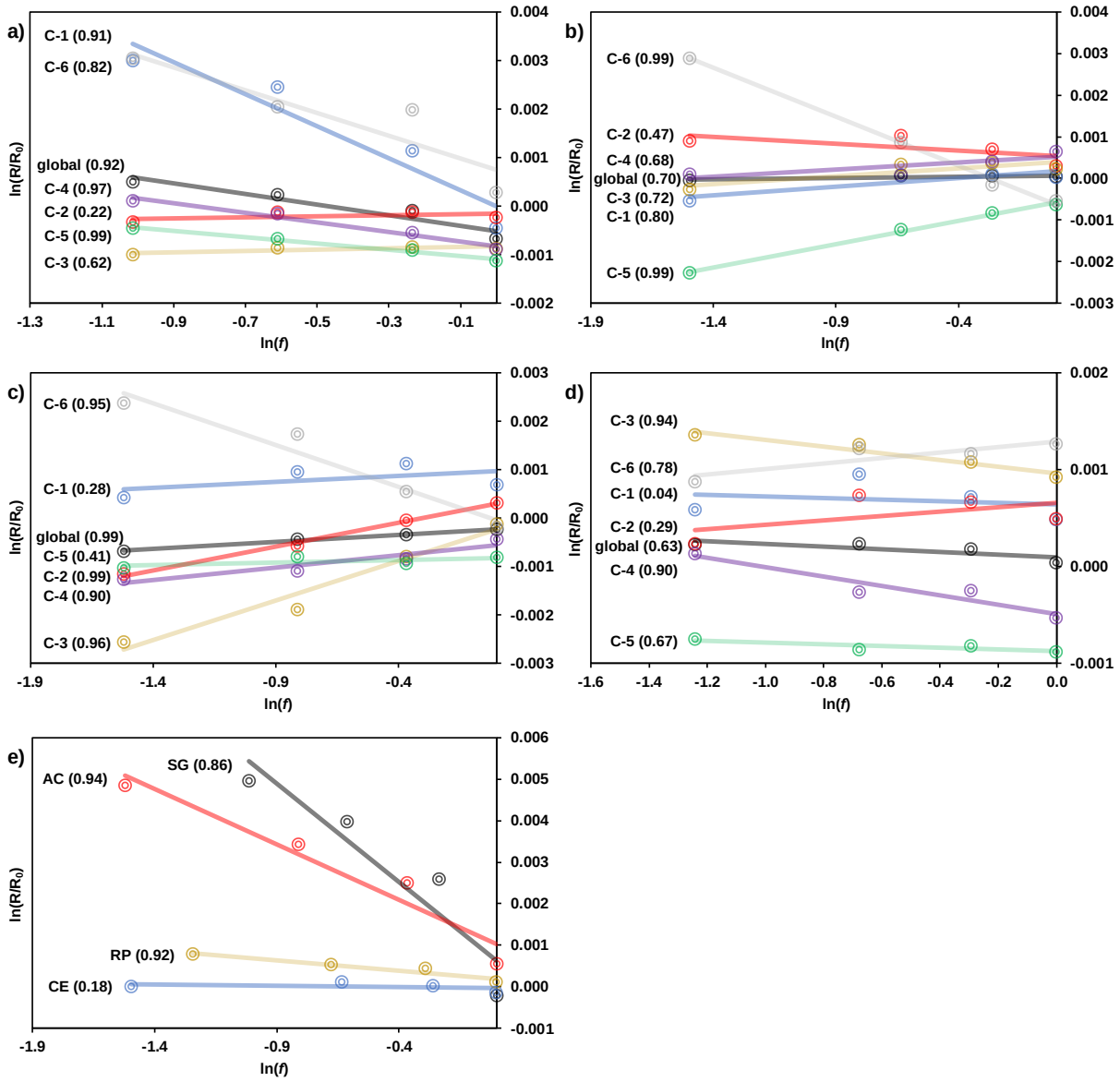

325

326 **Figure 3**: Rayleigh plots drawn using global and intramolecular (C-1 to C-6) ^{13}C experimental data
327 for migration in (a) normal phase silica gel, (b) cellulose, (c) activated charcoal and (d) reversed
328 phase silica gel. (e) Rayleigh plots drawn for ^{15}N data of the migration in each studied material
329 (SG: normal phase silica gel, CE: cellulose, AC: activated charcoal and RP: reversed phase silica gel.
330 Numbers in parentheses indicate the coefficient of determination (R^2) of each trend-line.

331

Both ^{13}C intramolecular and ^{15}N enrichment factors measured during the migration of paracetamol through the four studied stationary phases (silica gel = SG; cellulose = CE; activated charcoal = AC and C8-reversed phase = RP) are presented in this section and summarized in Table 3. As detailed in section 2.5, isotope effects are considered as normal (molecules containing light isotopes are preferentially eluted) when $\varepsilon < 0$ and inverse (heavy isotopologues are less retained in the column) when $\varepsilon > 0$.

Table 3: Enrichment factors (ε in ‰) obtained from irm-EA/MS (bulk) and from irm-^{13}C NMR (position-specific, C-1 to C-6) upon migration of paracetamol through the different solid phases as described in experimental section (SG = silica gel; CE = cellulose; AC = activated charcoal and RP = silica gel C8-reversed). The values shown after "±" are the expanded uncertainties of (U in ‰).

	ε (‰)							
	C_{bulk}	**C-1**	**C-2**	**C-3**	**C-4**	**C-5**	**C-6**	**N_{bulk}**
SG	-1.1 ± 0.5	-3.3 ± 1.5	+0.1 ± 0.3	+0.1 ± 0.1	-1.0 ± 0.2	-0.6 ± 0.1	-2.3 ± 1.6	-4.7 ± 2.5
CE	+0.1 ± 0.1	+0.4 ± 0.3	-0.3 ± 0.5	+0.4 ± 0.3	+0.3 ± 0.3	+1.1 ± 0.1	-2.4 ± 0.2	-0.1 ± 0.2
AC	+0.3 ± 0.0	+0.2 ± 0.6	+1.0 ± 0.1	+1.6 ± 0.5	+0.5 ± 0.3	+0.1 ± 0.2	-1.7 ± 0.6	-2.7 ± 0.9
RP	-0.1 ± 0.1	-0.1 ± 0.5	+0.2 ± 0.5	-0.3 ± 0.1	-0.5 ± 0.2	-0.1 ± 0.1	+0.3 ± 0.2	-0.5 ± 0.2

The link between observed IEs and the intermolecular interactions occurring between paracetamol and each considered stationary phase is discussed using their chemical structures described in Figure 2.In addition, previously published data obtained during the migration of

347 vanillin through SG [12] and RP [27] were treated using the method described in section 2.5 and
348 summarized in Table 4 and were included in the discussion.

349

350 **Table 4:** Enrichment factors (ε in ‰) obtained from irm-EA/MS (bulk) and from irm-^{13}C NMR
351 (position-specific, C-1 to C-8) upon migration of vanillin through silica gel (SG, Botosoa *et al.* 2009)
352 and reversed phase silica gel RP-18 (RP, Höhener *et al.* 2012). The values shown after "±" are the
353 expanded uncertainties of (U in ‰), at 95% confident level.

354

	ε (‰)								
	C_{bulk}	**C-1**	**C-2**	**C-3**	**C-4**	**C-5**	**C-6**	**C-7**	**C-8**
SG	-0.9 ± 0.1	-3.3 ± 0.6	+1.5 ± 0.4	-1.5 ± 0.2	-3.4 ± 0.2	-2.5 ± 0.4	+2.4 ± 0.3	-1.3 ± 0.2	-0.9 ± 0.1
RP	+0.3 ± 0.3	+0.6 ± 0.6	+1.1 ± 0.2	+0.7 ± 0.5	+0.4 ± 0.8	+0.3 ± 0.1	+0.3 ± 0.4	+0.2 ± 0.4	+0.3 ± 0.3

355

356

357 *3.3.1. Normal phase silica gel (SG)*

358 The migration of paracetamol in SG (Table 3) is associated with a small global ^{13}C normal isotope
359 effect of -1.1 ± 0.5‰. This result agrees with previous data obtained during the migration of
360 vanillin on this stationary phase (-0.9 ± 0.1‰, Table 4) where ^{13}C-depleted isotopologues are less
361 retained in the stationary phase (preferentially eluted). The presence of ^{13}C within paracetamol
362 molecules seems to result in a higher retention of heavy isotopologues. The PSIA revealed that
363 this IE is not equitably distributed between the carbon positions with a maximum ε located on C-
364 1 (-3.3 ± 1.5‰). The presence of a strong PSIE on this carbon position can be explained by the

presence of hydrogen-bonds between the oxygen of the acetamide function of paracetamol and acid hydrogens of silanols in SG (see Figure 2). The measurement of a smaller ε on carbon 6 (-2.3 ± 1.6‰) could be due to a secondary PSIE associated with the described interaction. This deduction is reinforced by the presence of a strong normal ^{15}N (-4.7 ± 2.5‰) IE during the migration which could be associated with the interaction of hydrogens from silica gel and the electron lone pair of the nitrogen atom. Other normal PSIEs located on the aromatic cycle of paracetamol (carbon positions 4 and 5) may be due to interactions between π electrons and the stationary phase during the elution. Surprisingly, no significant PSIE is measured on the C-2 of paracetamol although interactions between this chemical function and silica gel were anticipated. Intramolecular ^{13}C isotope data from migration of vanillin in SG are in accordance with these observations with the presence of a strong normal isotope effect on the carbon bearing the aldehyde function (-3.3 ± 0.6‰) and a smaller one on the methoxy group (-0.9 ± 0.1‰). The carbon of the aromatic cycle bearing the alcohol function (C-2) presents an inverse isotope effect (+1.5 ± 0.4‰) while no significant IE was observed on C-2 of paracetamol. Also, the amplitude of IEs within the aromatic cycle is higher in the case of vanillin with normal isotope effects with ε values comprised between -1.5 ± 0.2 and -3,4 ± 0.2‰ and an important inverse IE on C-6 (+2.4 ± 0.3‰).

More generally, the migration of these compounds through a polar stationary phase is associated with a strong normal ^{13}C IE inequitably distributed between the carbon positions because of the presence of polar chemical functions (here acetamide, alkoxy, aldehyde and alcohol) and their likely contribution to hydrogen bonds set up with the stationary phase.

3.3.2. Cellulose (CE)

Paracetamol migration in CE does not show any significant ^{13}C ε_g but PSIA revealed the contribution of both normal and inverse PSIEs on the different carbon positions of the molecule. In contrast to the SG experiment, the migration of paracetamol in CE is associated with a small inverse PSIE located on the C-1 (+0.4 ± 0.3‰). Surprisingly, a normal PSIE is detected on the C-6 (ε = -2.4 ± 0.2‰) which suggests that the presence of a ^{13}C on this carbon position may stabilize the interaction between the oxygen of the acetamide function of paracetamol and those from CE (Figure 3) resulting in a slower elution of the observed isotopomer. Nevertheless, no significant ^{15}N isotope fractionation is detected during this experiment. Other carbon positions (3 and 5) present positive ε values demonstrating that the presence of ^{12}C in the aromatic cycle leads to less stable interactions between paracetamol and CE.

3.3.3. Activated charcoal (AC)

The migration through AC is associated with a small inverse global IE (+0.3 ± 0.0‰), which is due to the counteractive contribution of both normal and inverse PSIEs within the molecule. As explained in the introduction, only weak non-covalent interactions (i.e. van der Waals and π-stacking) between paracetamol and activated charcoal are expected. A few significant PSIEs are detected in this case such as a normal PSIE on the C-6 (ε = -1.7 ± 0.6‰), which could be explained by the presence of a van der Waals interaction involving this methyl position of paracetamol. A normal PSIE here suggests that van der Waals interactions can be stabilized by the presence of ^{13}C, so isotopomers with a ^{12}C on C-6 will elute faster. Then, carbon positions 2, 3 and 4, located in the aromatic cycle, present inverse PSIEs of +1.0 ± 0.1‰, +1.6 ± 0.5‰ and +0.5 ± 0.3‰ respectively. These observed PSIEs may be due to the π-stacking interactions between paracetamol and aromatic functions in activated charcoal (Figure 2). According to these data, the

409 presence of ^{13}C on these carbon positions may stabilize the proposed intermolecular interaction
410 and induce isotope fractionation during migration. A significant normal ^{15}N IE is also detected
411 during the migration of paracetamol in activated charcoal (ε = -2.7 ± 0.9‰), which could be due
412 to the presence of van der Waals interaction between activated charcoal and this moiety of
413 paracetamol.

414 *3.3.4. Silica gel C8-reversed phase (RP)*

415 No significant ^{13}C global IE was detected during the migration of paracetamol on RP and only small
416 intramolecular PSIEs were identified. Previous data obtained from the migration of vanillin on RP
417 also showed a non-significant global IE (see Table 4). A small inverse PSIE was measured on C-6
418 of paracetamol (ε = +0.3 ± 0.2‰) which suggests that van der Waals interactions between this
419 methyl position and C_8 carbon chains from the stationary phase may be strengthened by the
420 presence of a ^{12}C on C-6, so isotopomers with a ^{13}C on this carbon position are preferentially
421 eluted. Conversely, ε of -0.3 ± 0.1 ‰ and -0.5 ± 0.2‰ are measured on C-3 and C-4, respectively,
422 so the presence of ^{13}C within the aromatic cycle of paracetamol seems to increase the retention
423 of the considered isotopomers on this stationary phase. A few significant inverse IEs are observed
424 within vanillin with +0.3 ± 0.1‰ on C-5, +0.7 ± 0.5‰ on C-3 and +1.1 ± 0.2‰ on C-2. This last
425 isotope effect has a higher amplitude than those observed in paracetamol, but the experimental
426 conditions used in the present study differed (reversed phase of type C_8 instead of type C_{18},
427 different eluents, different compounds studied).

428 However, the migration of such polar compounds through nonpolar stationary phases seems to
429 be associated with only a few small inverse isotope effects.

3.3.5. Intramolecular ε associated with non-covalent interactions

According to data obtained in the present study, the chemical composition of the solid medium traversed by an organic pollutant has an influence on the associated isotope fractionation. Note that the same eluent mixture is used during each chromatography experiments so the IEs potentially created by interactions between eluent and paracetamol are hidden. In this context, the ε values measured for each matrix can be used to discuss the link between observed NCIEs and the chemical structure of the stationary phase. These results suggest that intermolecular interactions established between the substrate (here paracetamol and vanillin) and the soil (modeled by various stationary phases in this study) have a direct influence on the selectivity of isotopomers preferentially migrating. The PSIEs associated with the migration experiments allowed the identification of the isotopomers that preferentially interact with each of the tested stationary phases. The presence of small or non-significant global IEs (measured using irm-MS) is proved to be due to the counteractive contribution of both normal and inverse intramolecular PSIEs (measured by irm-^{13}C NMR) for different carbon positions of the substrate.

The key point of the present study is the association of the non-covalent interactions between the stationary phase and the substrate with the resulting intramolecular PSIEs. As an example, both SG and CE are polar, so hydrogen-bonds between these stationary phases and paracetamol or vanillin can be made. The presence of PSIEs on C-1 associated with the migration through these two materials confirms the presence of hydrogen bonds between acidic hydrogens of the phases and the oxygen atom of the acetamide function (Table 3). Thus, it can be predicted that when a polar organic contaminant migrates in a soil containing polar phases, isotope fractionation on the carbon positions bearing a polar function (alcohol, ketone...) will occur. The presence of

452 intramolecular IEs associated with the formation of hydrogen bonds has already been proven to
453 be directly correlated in the case of evaporation of VOCs [14]. Conversely, no PSIEs should be
454 observed on polar functions during the migration in non-polar medium such as AC or RP.

455 The presence of weak interactions, such as van de Waals forces or π-stacking, can also induce
456 PSIEs but it is much more difficult to discuss any direct implication in the distribution of PSIEs
457 because they do not involve a specific chemical function of the substrate. The exact chemical
458 structure of AC is not well defined, but the presence of aromatic cycles is expected in this material.
459 Thus, it is not surprising that significant PSIEs at carbon positions located in the aromatic cycle of
460 paracetamol and vanillin (Tables 3 and 4) are observed. However, isotope fractionation is also
461 observed on carbon positions of the aromatic cycle during the migration of paracetamol through
462 the other stationary phases which may be due to (i) interactions between the π electrons and
463 acidic hydrogens from SG and CE or (ii) hydrophobic interaction with the C_8 aliphatic chain of the
464 RP. Similarly, it is hard fully to interpret the significant isotope effect observed on C-6 of
465 paracetamol and C-8 of vanillin in all experiments (Table 2). This PSIEs could be considered as a
466 secondary isotope effect due to the presence of hydrogen bonds on the C=O or the O of ether
467 function for paracetamol and vanillin respectively (for SG and CE) or a direct van der Waals
468 interaction in the case of the non-polar media (AC and RP). Further research is required to resolve
469 these problems.

470 Moreover, these data directly demonstrate the value of intramolecular isotope analysis to study
471 further the origin and fate of organic pollutants. As PSIEs are different depending on the traversed
472 stationary phase, modeling the isotope fractionation occurring during migration in pure material

associated with the chemical analysis of the contaminated soil could help tracing organic pollutants in the environment.

3.3.6. Theoretical calculations of the enrichment factors.

Theoretical prediction of heavy-atom isotope effects poses numerous problems since they are usually very small. Reported herein experimental results, obtained for different solid phases, provided a unique opportunity to evaluate quality of different theoretical models used in quantum-chemical calculations of isotope effects associated with changes in weak interactions. The obtained results are collected in Table 5.

Table 5: Enrichment factors (ε in ‰) obtained from quantum mechanical calculations for transition from diethyl ether to aqueous solution (14aq), gas phase, and acetone.

	ε (‰)							
	C_{bulk}	**C-1**	**C-2**	**C-3**	**C-4**	**C-5**	**C-6**	**N_{bulk}**
14aq	-1.0	-1.6	0.0	-0.9	-0.8	-0.8	-1.9	-4.9
gas	+0.2	+1.2	0.0	+0.5	-0.1	0.0	-0.7	-0.9
acetone	+0.3	+0.8	+0.6	+0.3	+0.4	+0.1	0.0	-0.2

The two first entries in Table 5 represent fractionations calculated for the process of going from diethyl ether solution either to very polar and hydrogen-bonded environment (aq14) or to the gas phase. As can be seen, except for the value for the C3 position, results obtained using aq14 model are in very good agreement with the experimental results for SG (normal phase silica gel). We have tried to rationalize this single discrepancy, however, no clear indication of its source has

been identified based on the geometrical features and electrostatic properties. The gas phase model, on the other hand, agrees well with those obtained for the other three solid phases although not with particular single one. We have, therefore, calculated a putative process of paracetamol changing phases by going from pure ethyl ether to acetone. These values might reflect preferential solvation and can be treated as uncertainty on the calculated values.

Results collected in Table 3 seem to implicate that the polarity effects dominate over specific hydrogen bonding interactions since the results obtained for cellulose support are much closer to those of activated carbon and reverse phase than to those obtained for silica gel. Thus the results obtained with the apparent solvent model indicate that the presence of the explicit hydrogen bonding between the paracetamol and solvent molecules of high polarity of the solvent shell environment results in strong polarization that affects the isotopic fractionation. On the contrary, when continuum models of solvent are used accounting for these polarization effects is much weaker leading to lower values of isotopic fractionation.

4. Conclusions

The data presented confirm IEs associated with the migration of organic compounds such as paracetamol, and that the extent of these depend on the matrix through which the considered chemical is migrating. These results also confirm that when the recovery of a target compound is not total during isolation by liquid chromatography, its isotope composition may be affected, especially when followed by intramolecular isotope analysis. Then, the corrections of the measured isotope data need to consider the chemical composition of both the stationary phase

511 and the isolate molecule in addition to amount of lost compound (see Rayleigh plots). A better
512 understanding of these “binding isotope effects” should help describing the processes involved
513 in liquid chromatography and, more generally, in migration experiments. Hence, these results
514 endorse the need to take the migration into account while studying the isotope composition of
515 organic contaminants during their remediation. Furthermore, the use of intramolecular isotope
516 analysis is potentially of considerable benefit for environmental forensic investigations, as they
517 give indications of the type of matrix through which the pollutant has migrated. The identification
518 of PSIEs associated with migration experiments should help in understanding the link between
519 the transport of an organic contaminant and the chemical composition of the soil. This is the main
520 objective of the present work. Understanding the mechanisms involved is essential to developing
521 detailed transport models for the prediction of the intramolecular of isotope distribution within
522 an organic contaminant and its evolution in the environment. As sorption is considered one of
523 the most promising method to eliminate organic pollutants from water [54,55] the determination
524 of the PSIEs associated with this process should lead to a better understanding of the mechanisms
525 involved, hence aid making contaminant monitoring more efficient. Thus, they provide further
526 insight of value for the characterization of the source(s) and the detection/quantification of
527 remediation mechanisms. Unfortunately, as NMR has a low sensitivity, large quantities of pure
528 compound are required to perform PSIA on field samples. However, recent advances in NMR are
529 making it possible to access the intramolecular ^{13}C isotope composition using much lower
530 quantities [56], while other PSIA methods using on-line pyrolysis coupled with irm-MS [22,57] or
531 high resolution MS [22] are offering opportunities for similar detail to be obtained on much
532 smaller samples still. Such approaches should make possible experiments in real soil conditions

aimed at understanding and modeling the exact link between intermolecular non-covalent interactions and intramolecular isotope distributions within target molecules. Also, the great agreement between PSIEs measured by ^{13}C-NMR and those calculated using theoretical models demonstrate the great potential of quantum mechanics for predicting the evolution of intramolecular isotopic composition of organic environmental contaminants. Future developments of more sensitive intramolecular isotope analysis methods associated with theoretical calculations should provide excellent tools to trace the origin and fate of organic compounds detected in environment.

Supplementary material

Supporting information is added to this article, see “Supporting_Information.xlsx”.

Funding

This work is funded by the French National Research Agency ANR, project ISOTO-POL funded by the program CESA (no. 009 01). The access to PL-Grid computing resources at Cyfronet is gratefully acknowledged.

Acknowledgements

M.J. thanks the ANR for funding his PhD bursary through the ISOTO-POL project and Kiban S for funding his postdoctoral fellowship (Grant-in-Aid for Scientific Research S, 23224013, MEXT, Japan). We thank Dr. Richard J. Robins for his help with language correction of this article.

References

1. Tanaka, N.; Thornton, E.R. Isotope effects in hydrophobic binding measured by high-pressure liquid chromatography. *J. Am. Chem. Soc.* **1976**, *98*, 1617–1619, doi:10.1021/ja00422a076.
2. Wade, D. Deuterium isotope effects on noncovalent interactions between molecules. *Chem. Biol. Interact.* **1999**, *117*, 191–217, doi:10.1016/S0009-2797(98)00097-0.
3. Turowski, M.; Yamakawa, N.; Meller, J.; Kimata, K.; Ikegami, T.; Hosoya, K.; Tanaka, N.; Thornton, E.R. Deuterium Isotope Effects on Hydrophobic Interactions: The Importance of Dispersion Interactions in the Hydrophobic Phase. *J. Am. Chem. Soc.* **2003**, *125*, 13836–13849, doi:10.1021/ja036006g.
4. Godin, J.-P.; McCullagh, J.S.O. Review: Current applications and challenges for liquid chromatography coupled to isotope ratio mass spectrometry (LC/IRMS). *Rapid Commun. Mass Spectrom.* **2011**, *25*, 3019–3028, doi:10.1002/rcm.5167.
5. Meier-Augenstein, W. Applied gas chromatography coupled to isotope ratio mass spectrometry. *J. Chromatogr. A* **1999**, *842*, 351–371, doi:10.1016/S0021-9673(98)01057-7.
6. Benson, S.; Lennard, C.; Maynard, P.; Roux, C. Forensic applications of isotope ratio mass spectrometry—A review. *Forensic Sci. Int.* **2006**, *157*, 1–22, doi:10.1016/j.forsciint.2005.03.012.

7. Schmidt, T.C.; Zwank, L.; Elsner, M.; Berg, M.; Meckenstock, R.U.; Haderlein, S.B. Compound-specific stable isotope analysis of organic contaminants in natural environments: a critical review of the state of the art, prospects, and future challenges. *Anal. Bioanal. Chem.* **2004**, *378*, 283–300, doi:10.1007/s00216-003-2350-y.
8. Elsner, M.; Jochmann, M.A.; Hofstetter, T.B.; Hunkeler, D.; Bernstein, A.; Schmidt, T.C.; Schimmelmann, A. Current challenges in compound-specific stable isotope analysis of environmental organic contaminants. *Anal. Bioanal. Chem.* **2012**, *403*, 2471–91, doi:10.1007/s00216-011-5683-y.
9. Chiogna, G.; Eberhardt, C.; Grathwohl, P.; Cirpka, O.A.; Rolle, M. Evidence of Compound-Dependent Hydrodynamic and Mechanical Transverse Dispersion by Multitracer Laboratory Experiments. *Environ. Sci. Technol.* **2010**, *44*, 688–693, doi:10.1021/es9023964.
10. Van Breukelen, B.M.; Rolle, M. Transverse Hydrodynamic Dispersion Effects on Isotope Signals in Groundwater Chlorinated Solvents' Plumes. *Environ. Sci. Technol.* **2012**, *46*, 7700–7708, doi:10.1021/es301058z.
11. Jin, B.; Rolle, M.; Li, T.; Haderlein, S.B. Diffusive Fractionation of BTEX and Chlorinated Ethenes in Aqueous Solution: Quantification of Spatial Isotope Gradients. *Environ. Sci. Technol.* **2014**, *68*, 6141–6150.
12. Botosoa, E.P.; Silvestre, V.; Robins, R.J.; Rojas, J.M.M.; Guillou, C.; Remaud, G.S. Evidence of ^{13}C non-covalent isotope effects obtained by quantitative ^{13}C nuclear magnetic resonance spectroscopy at natural abundance during normal phase liquid chromatography. *J. Chromatogr. A* **2009**, *1216*, 7043–7048, doi:10.1016/j.chroma.2009.08.066.

13. Thullner, M.; Centler, F.; Richnow, H.-H.; Fischer, A. Quantification of organic pollutant degradation in contaminated aquifers using compound specific stable isotope analysis – Review of recent developments. *Org. Geochem.* **2012**, *42*, 1440–1460, doi:10.1016/j.orggeochem.2011.10.011.
14. Julien, M.; Höhener, P.; Robins, R.J.; Parinet, J.; Remaud, G.S. Position-Specific ^{13}C Fractionation during Liquid–Vapor Transition Correlated to the Strength of Intermolecular Interaction in the Liquid Phase. *J. Phys. Chem. B* **2017**, *121*, 5810–5817, doi:10.1021/acs.jpcb.7b00971.
15. Morasch, B.; Richnow, H.H.; Schink, B.; Meckenstock, R.U. Stable Hydrogen and Carbon Isotope Fractionation during Microbial Toluene Degradation: Mechanistic and Environmental Aspects | Applied and Environmental Microbiology. *Appl. Environ. Microbiol. 67*, 4842–4849.
16. Caytan, E.; Botosoa, E.P.; Silvestre, V.; Robins, R.J.; Akoka, S.; Remaud, G.S. Accurate Quantitative ^{13}C NMR Spectroscopy: Repeatability over Time of Site-Specific ^{13}C Isotope Ratio Determination. *Anal. Chem.* **2007**, *79*, 8266–8269, doi:10.1021/ac070826k.
17. Gilbert, A.; Robins, R.J.; Remaud, G.S.; Tcherkez, G.G. Intramolecular ^{13}C pattern in hexoses from autotrophic and heterotrophic C3 plant tissues. *Proc. Natl. Acad. Sci. U. S. A.* **2012**, *109*, 18204–9, doi:10.1073/pnas.1211149109.
18. Jézéquel, T.; Joubert, V.; Giraudeau, P.; Remaud, G.S.; Akoka, S. The new face of isotopic NMR at natural abundance. *Magn. Reson. Chem.* **2017**, *55*, 77–90, doi:10.1002/mrc.4548.
19. Corso, T.N.; Brenna, J.T. High-precision position-specific isotope analysis. *Proc. Natl. Acad. Sci.* **1997**, *94*, 1049–1053.

20. Yamada, K.; Tanaka, M.; Nakagawa, F.; Yoshida, N. On-line measurement of intramolecular carbon isotope distribution of acetic acid by continuous-flow isotope ratio mass spectrometry. *Rapid Commun. Mass Spectrom.* **2002**, *16*, 1059–64, doi:10.1002/rcm.678.
21. Gilbert, A.; Yamada, K.; Yoshida, N. Accurate Method for the Determination of Intramolecular ^{13}C Isotope Composition of Ethanol from Aqueous Solutions. *Anal. Chem.* **2013**, *85*, 6566–6570, doi:10.1021/ac401021p.
22. Gilbert, A.; Yamada, K.; Suda, K.; Ueno, Y.; Yoshida, N. Measurement of position-specific ^{13}C isotopic composition of propane at the nanomole level. *Geochim. Cosmochim. Acta* **2016**, *177*, 205–216, doi:10.1016/j.gca.2016.01.017.
23. Piasecki, A.; Sessions, A.; Lawson, M.; Ferreira, A.A.; Neto, E.V.S.; Eiler, J.M. Analysis of the site-specific carbon isotope composition of propane by gas source isotope ratio mass spectrometer. *Geochim. Cosmochim. Acta* **janvier 9**, *188*, 58–72, doi:10.1016/j.gca.2016.04.048.
24. Cesar, J.; Eiler, J.; Dallas, B.; Chimiak, L.; Grice, K. Isotope heterogeneity in ethyltoluenes from Australian condensates, and their stable carbon site-specific isotope analysis. *Org. Geochem.* **2019**, *135*, 32–37, doi:10.1016/j.orggeochem.2019.06.002.
25. Botosoa, E.P.; Caytan, E.; Silvestre, V.; Robins, R.J.; Akoka, S.; Remaud, G.S. Unexpected fractionation in site-specific ^{13}C isotopic distribution detected by quantitative ^{13}C NMR at natural abundance. *J. Am. Chem. Soc.* **2008**, *130*, 414–415, doi:10.1021/ja0771181.
26. Joubert, V.; Silvestre, V.; Lelièvre, M.; Ladroue, V.; Besacier, F.; Akoka, S.; Remaud, G.S. Position-specific ^{15}N isotope analysis in organic molecules: A high-precision ^{15}N NMR method

635 to determine the intramolecular ^{15}N isotope composition and fractionation at natural
636 abundance. *Magn. Reson. Chem.* **2019**, *57*, 1136–1142, doi:10.1002/mrc.4903.
637 27. Höhener, P.; Silvestre, V.; Lefrançois, A.; Loquet, D.; Botosoa, E.P.; Robins, R.J.; Remaud, G.S.
638 Analytical model for site-specific isotope fractionation in ^{13}C during sorption: Determination
639 by isotopic ^{13}C NMR spectrometry with vanillin as model compound. *Chemosphere* **2012**, *87*,
640 445–452, doi:10.1016/j.chemosphere.2011.12.023.
641 28. Julien, M.; Parinet, J.; Nun, P.; Bayle, K.; Höhener, P.; Robins, R.J.; Remaud, G.S. Fractionation
642 in position-specific isotope composition during vaporization of environmental pollutants
643 measured with isotope ratio monitoring by ^{13}C nuclear magnetic resonance spectrometry.
644 *Environ. Pollut.* **2015**, *205*, 299–306, doi:10.1016/j.envpol.2015.05.047.
645 29. Julien, M.; Nun, P.; Robins, R.J.; Remaud, G.S.; Parinet, J.; Höhener, P. Insights into
646 Mechanistic Models for Evaporation of Organic Liquids in the Environment Obtained by
647 Position-Specific Carbon Isotope Analysis. *Environ. Sci. Technol.* **2015**, *49*, 12782–12788,
648 doi:10.1021/acs.est.5b03280.
649 30. Zhang, B.-L.; Jouitteau, C.; Pionnier, S.; Gentil, E. Determination of Multiple Equilibrium
650 Isotopic Fractionation Factors at Natural Abundance in Liquid-Vapor Transitions of Organic
651 Molecules. *J. Phys. Chem. B* **2002**, *106*, 2983–2988, doi:10.1021/jp013522p.
652 31. Harrington, R.R.; Poulson, S.R.; Drever, J.I.; Colberg, P.J.S.; Kelly, E.F. Carbon isotope
653 systematics of monoaromatic hydrocarbons: vaporization and adsorption experiments. *Org.*
654 *Geochem.* **1999**, *30*, 765–775, doi:10.1016/S0146-6380(99)00059-5.
655 32. Kopinke, F.-D.; Georgi, A.; Voskamp, M.; Richnow, H.H. Carbon Isotope Fractionation of
656 Organic Contaminants Due to Retardation on Humic Substances: Implications for Natural

Attenuation Studies in Aquifers. *Environ. Sci. Technol.* **2005**, *39*, 6052–6062, doi:10.1021/es040096n.

33. Schüth, C.; Taubald, H.; Bolaño, N.; Maciejczyk, K. Carbon and hydrogen isotope effects during sorption of organic contaminants on carbonaceous materials. *J. Contam. Hydrol.* **2003**, *64*, 269–281, doi:10.1016/S0169-7722(02)00216-4.
34. Slater, G.F.; Ahad, J.M.E.; Sherwood Lollar, B.; Allen-King, R.; Sleep, B. Carbon Isotope Effects Resulting from Equilibrium Sorption of Dissolved VOCs. *Anal. Chem.* **2000**, *72*, 5669–5672, doi:10.1021/ac000691h.
35. Imfeld, G.; Kopinke, F.D.; Fischer, A.; Richnow, H.H. Carbon and hydrogen isotope fractionation of benzene and toluene during hydrophobic sorption in multistep batch experiments. *Chemosphere* **2014**, *107*, 454–461, doi:10.1016/j.chemosphere.2014.01.063.
36. Granberg, R.A.; Rasmuson, Å.C. Solubility of Paracetamol in Pure Solvents. *J. Chem. Eng. Data* **1999**, *44*, 1391–1395, doi:10.1021/je990124v.
37. Silvestre, V.; Mboula, V.M.; Jouitteau, C.; Akoka, S.; Robins, R.J.; Remaud, G.S. Isotopic ^{13}C NMR spectrometry to assess counterfeiting of active pharmaceutical ingredients: Site-specific ^{13}C content of aspirin and paracetamol. *J. Pharm. Biomed. Anal.* **2009**, *50*, 336–341, doi:10.1016/j.jpba.2009.04.030.
38. Akoka, S.; Remaud, G.S. NMR-based isotopic and isotopomic analysis. *Prog. Nucl. Magn. Reson. Spectrosc.* **2020**, *120–121*, 1–24, doi:10.1016/j.pnmrs.2020.07.001.
39. Elsner, M.; McKelvie, J.; Lacrampe Couloume, G.; Sherwood Lollar, B. Insight into Methyl tert-Butyl Ether (MTBE) Stable Isotope Fractionation from Abiotic Reference Experiments. *Environ. Sci. Technol.* **2007**, *41*, 5693–5700, doi:10.1021/es070531o.

679 40. Höhener, P.; Atteia, O. Rayleigh equation for evolution of stable isotope ratios in contaminant
680 decay chains. *Geochim. Cosmochim. Acta* **2014**, *126*, 70–77, doi:10.1016/j.gca.2013.10.036.
681 41. Julien, M.; Gilbert, A.; Yamada, K.; Robins, R.J.; Höhener, P.; Yoshida, N.; Remaud, G.S.
682 Expanded uncertainty associated with determination of isotope enrichment factors:
683 Comparison of two point calculation and Rayleigh-plot. *Talanta* **2018**, *176*, 367–373,
684 doi:10.1016/j.talanta.2017.08.038.
685 42. Marenich, A.V.; Cramer, C.J.; Truhlar, D.G. Universal Solvation Model Based on Solute Electron
686 Density and on a Continuum Model of the Solvent Defined by the Bulk Dielectric Constant and
687 Atomic Surface Tensions. *J. Phys. Chem. B* **2009**, *113*, 6378–6396, doi:10.1021/jp810292n.
688 43. Chai, J.-D.; Head-Gordon, M. Long-range corrected hybrid density functionals with damped
689 atom–atom dispersion corrections. *Phys. Chem. Chem. Phys.* **2008**, *10*, 6615–6620,
690 doi:10.1039/B810189B.
691 44. Weigend, F.; Ahlrichs, R. Balanced basis sets of split valence, triple zeta valence and quadruple
692 zeta valence quality for H to Rn: Design and assessment of accuracy. *Phys. Chem. Chem. Phys.*
693 **2005**, *7*, 3297–3305, doi:10.1039/B508541A.
694 45. Frisch, M.J.; Trucks, G.W.; Schlegel, H.B. et al. *Gaussian 16, Revision C.01*; Gaussian, Inc.,
695 Wallingford CT, 2016;
696 46. Klajman, K.; Dybala-Defratyka, A.; Paneth, P. Computational Investigations of Position-Specific
697 Vapor Pressure Isotope Effects in Ethanol—Toward More Powerful Isotope Models for Food
698 Forensics. *ACS Omega* **2020**, *5*, 18499–18506, doi:10.1021/acsomega.0c02446.
699 47. Anisimov, V.; Paneth, P. A program for studies of isotope effects using Hessian modifications.
700 *J. Math. Chem.* **1999**, *26*, 75–86, doi:10.1023/A:1019173509273.

48. Graham, G.G.; Scott, K.F. Mechanism of Action of Paracetamol. *Am. J. Ther.* **2005**, *12*, 46–55.
49. Bedner, M.; MacCrehan, W.A. Transformation of Acetaminophen by Chlorination Produces the Toxicants 1,4-Benzoquinone and N-Acetyl-p-benzoquinone Imine. *Environ. Sci. Technol.* **2006**, *40*, 516–522, doi:10.1021/es0509073.
50. Moore, M.; Thor, H.; Moore, G.; Nelson, S.; Moldéus, P.; Orrenius, S. The toxicity of acetaminophen and N-acetyl-p-benzoquinone imine in isolated hepatocytes is associated with thiol depletion and increased cytosolic Ca2+. *J. Biol. Chem.* **1985**, *260*, 13035–13040.
51. Thijssen, H.H.; Soute, B.A.; Vervoort, L.M.; Claessens, J.G. Paracetamol (acetaminophen) warfarin interaction: NAPQI, the toxic metabolite of paracetamol, is an inhibitor of enzymes in the vitamin K cycle. *Thromb. Haemost.* **2004**, *92*, 797–802, doi:10.1160/TH04-02-0109.
52. Kalinec, G.M.; Thein, P.; Parsa, A.; Yorgason, J.; Luxford, W.; Urrutia, R.; Kalinec, F. Acetaminophen and NAPQI are toxic to auditory cells via oxidative and endoplasmic reticulum stress-dependent pathways. *Hear. Res.* **2014**, *313*, 26–37, doi:10.1016/j.heares.2014.04.007.
53. Remaud, G.; Giraudeau, P.; Lesot, P.; Akoka, S. Isotope Ratio Monitoring by NMR. Part 1: Recent Advances. In *Modern Magnetic Resonance, 2nd Edition*; Webb, E.G., Ed.; Springer International Publishing, 2016.
54. Rossner, A.; Knappe, D.R.U. MTBE adsorption on alternative adsorbents and packed bed adsorber performance. *Water Res.* **2008**, *42*, 2287–2299.
55. Rossner, A.; Snyder, S.A.; Knappe, D.R.U. Removal of emerging contaminants of concern by alternative adsorbents. *Water Res.* **2009**, *43*, 3787–3796, doi:10.1016/j.watres.2009.06.009.

56. Joubert, V.; Silvestre, V.; Grand, M.; Loquet, D.; Ladroue, V.; Besacier, F.; Akoka, S.; Remaud, G.S. Full Spectrum Isotopic ^{13}C NMR Using Polarization Transfer for Position-Specific Isotope Analysis. *Anal. Chem.* **2018**, *90*, 8692–8699, doi:10.1021/acs.analchem.8b02139.
57. Julien, M.; Goldman, M.J.; Liu, C.; Horita, J.; Boreham, C.J.; Yamada, K.; Green, W.H.; Yoshida, N.; Gilbert, A. Intramolecular ^{13}C isotope distributions of butane from natural gases. *Chem. Geol.* **2020**, 119571, doi:10.1016/j.chemgeo.2020.119571.